

Comparison of the performance of inorganic ultrafiltration and organic nanofiltration membranes for removal of nitrate contamination of groundwater

M. Breida^{a,*}, W. Taanaoui^a, A. Karim^a, S. Alami Younssi^a, M. Ouammou^a,
A. Aaddane^a, Y.A. Boussouga^b, A. Lhassani^b

^aLaboratory of Materials, Faculty of Sciences and Technologies of Mohammedia, University Hassan II of Casablanca, P.O. Box: 146 Mohammedia 20650, Morocco, email: Breidamajda@gmail.com

^bLaboratory of Applied Chemistry, Faculty of Science and Technology of Fez, Sidi Mohamed Ben Abdellah University, P.O. Box: 2202 Fez, Morocco

Received 28 March 2020; Accepted 8 August 2020

ABSTRACT

Contamination from Moroccan agricultural activity and, specifically, nitrate (NO_3^-) pollution is a major concern in groundwater supervision. This study aims to compare inorganic ultrafiltration ($\gamma\text{-Al}_2\text{O}_3$) to organic nanofiltration membranes (NF90 and NF270 Dow/Filmtec, South Miami, USA) in terms of NO_3^- removal and permeate flux. The influence of experimental parameters (pH, applied pressure, ionic strength, and the variation of the chemical composition of feed solution) on the membranes' performance, onto NO_3^- removal, was studied. The influence of the associated cation was also highlighted. The filtration experiments were first carried out on synthetic solutions, then on groundwater from two different Moroccan regions. The experimental filtration results demonstrated that the UF membrane underscores its position in NO_3^- removal among organic membranes ($R(\text{NF90}) \% > R(\text{UF}) \% > R(\text{NF270})\%$). The NO_3^- rejection depends on pH. The best rejections for NF90 and NF270 are, respectively, in the order of 70% and 41% at pH above 8, while the best rejection of 60% is found for $\gamma\text{-Al}_2\text{O}_3$ UF at pH 7. The increase of NO_3^- concentration and multivalent anions, lead to a decrease in NO_3^- rejection. Ions' valency and hydrated radius, as well as, membrane-solute electrostatic interaction have a drastic effect on NO_3^- rejection. The NF90 has the highest rejections since the separation is caused by dual forces, charge, and size effects. The electrostatic interactions during tight UF are more pronounced than NF270. Denitrification of Sidi Taibi groundwater by NF90, UF, and NF270, amounts, respectively, to approximately 64%, 56%, and 20% for 6 bar and natural pH. The total mineralization of water influences drastically on NO_3^- removal.

Keywords: Organic membranes; Inorganic membranes; Ultrafiltration; Nanofiltration; Groundwater denitrification

1. Introduction

Water is crucial for human health and sustainable development. Yet, 2.4 billion people are deprived of clean water, while 946 million of people are compelled to drink contaminated water [1]. Groundwater sources, which covers 97% of global freshwater and serves as drinking water source for 50% of the world population, are in permanent risk of

contamination especially by pollutants from agricultural activities (e.g., nitrate (NO_3^-)) [2,3]. In Morocco, the agricultural activity is increasing over time and it can be valued at approximately 85,000 ha/y [4]. Fertilizers (mainly N-based fertilizers) are well known as an integral part of agricultural production, and are reported as one of the primary factor leading to NO_3^- pollution [2,5,6]. NO_3^- pollution of Moroccan

* Corresponding author.

water via fertilizers was reported for many basins. The contamination of the Souss-Massa Bassin, the Loukkos, Essaouira, and the basin of Triffa plain in north-east Morocco was confirmed respectively by Laftouhi et al. [7], Fetouani et al. [8], and Mourabit et al. [9]. NO_3^- is a compound of nitrogen (N) found in nature which presents the most stable form of N. N is transformed to ammonia that in turn is converted to nitrite (NO_2^-) and NO_3^- . NO_3^- is characterized by high solubility and mobility with little sorption. Further, NO_3^- ions are readily washed into the body of surface water (by runoff or via soil infiltration). The high levels of NO_3^- concentration in groundwater are related to many harmful effects [2]. The consumption of NO_3^- has been correlated to hypertension, methemoglobinemia in children, thyroid malfunctioning, and the risk of stomach cancer diseases [5,10]. NO_3^- in groundwater is also related to environmental threats such as eutrophication and seasonal hypoxia [10,11]. In order to restore the quality of underground water and deter hazards to mankind, various approaches have been targeted in terms of legislation and water decontamination techniques. According to the Moroccan standard for surveillance and monitoring the water in public supply networks, the admitted level of NO_3^- is 50 mg/L. This limit is in accordance with the guidelines for Canadian drinking water quality, as well as with the world health organization's recommendations, who have fixed the maximum acceptable concentration at 10 mg/L NO_3^- -N (which corresponds to 45–50 mg/L of NO_3^-) [2,5,11]. Several management practices have been applied to reduce NO_3^- concentration, for instance, the use of improved fertilizers and controlled drainage [12]. Nevertheless, the efforts made in terms of management remain insufficient to overcome the NO_3^- problem. As a result, different methods have been used to reduce the pollution of water. According to Breida et al. [2], the classical processes applied for NO_3^- removal in drinking water are electrodialysis, biological denitrification, and ion exchange [12]. NO_3^- conventional treatment processes are known to be complex to execute. Membrane technology, especially pressure-driven membranes (reverse osmosis (RO), nanofiltration (NF), ultrafiltration (UF), and microfiltration (MF)), has become a promising industrial alternative compared with traditional treatment techniques [2,5,13]. The efficiency of pollutants removal by membrane processes depends on the type of membrane and the operating conditions of the system. Membranes are divided (based on material nature) into two categories, organic (or polymeric) and inorganic (or ceramic/mineral) membranes. The development of organic membranes is advancing at a sustained pace, while inorganic membranes have gained growing interest. Organic NF membranes demonstrate some drawbacks, such as fouling compared to UF ceramic membrane. Fouling of NF organic membranes increases the process costs caused by an increase in energy demand and maintenance [14]. While inorganic UF membranes require an excessive manufacturing cost [15]. From maintenance and economical point of view, the use of inorganic membranes is more recommended due to their thermal, mechanical, chemical stability, and prolonged lifetime [13,16,17]. One of the remaining challenges in NF organic membrane is the quantitative understanding of the relationship between NF membrane's structure, separation performance, and

feed solution chemistry [18]. The use of $\gamma\text{-Al}_2\text{O}_3$ UF membrane for NO_3^- removal was demonstrated and confirmed by Breida et al. [5]. The main objectives of this study are to (i) improve the use of $\gamma\text{-Al}_2\text{O}_3$ UF through its application in NO_3^- removal from Moroccan agricultural groundwater, (ii) to strengthen its position against organic membranes (two NF membranes (NF90 and NF270)). Detailed characterization of the three membranes in terms of wettability and permeability was investigated. The influence of parameters (pH, applied pressure (ΔP), ionic strength, and the variation of the chemical composition of the studied solutions) on NO_3^- rejection by the three membranes were studied. In this study, the denitrification of underground water from two distinct regions in Morocco was studied and discussed.

2. Experimental methodology

2.1. Materials

2.1.1. Studied membranes

In the present study, the efficiency of two commercial polyamides NF membranes (flat sheet NF90 and NF270) in NO_3^- removal was tested and compared with a UF ($\gamma\text{-Al}_2\text{O}_3$) inorganic membrane. The tubular UF membrane was manufactured by Pall Corporation (Saint-Germain-en-Laye, France) while the two NF membranes were manufactured by Dow/FilmTec (South Miami, USA). The characteristics of the three membranes are reported in Table 1.

The NF membranes have an asymmetric and composite structure. NF membranes are composed of an active layer, made of aromatic polyamide, and deposited on polyester support through a microporous polysulfone interlayer. The active layer of NF90 consists of a fully aromatic polyamide while NF270 holds a very thin semi-aromatic piperazine-based polyamide active layer [24–26].

The UF membrane has an active layer of $\gamma\text{-Al}_2\text{O}_3$ deposited on a MF support made of $\alpha\text{-Al}_2\text{O}_3$. Prior to filtration, the three membranes were immersed in pure water (18.2 M Ω -cm) for 48 h, to facilitate the flow passage and remove any preservative agents from membranes.

2.1.2. Moroccan study areas

The performance of membranes was evaluated and compared through (i) the filtration of different synthetic solutions, and (ii) underground water from two distinct regions in Morocco. The natural water from the two wells is classified as NO_3^- vulnerable zones. The geographical setting of the distinct study areas is presented in Fig. 1. The compositions of the wells' water, well 1 (P1) from the Fedalate commune and well 2 (P2) from the Sidi Taibi commune, are reported in Table 2.

2.1.3. Chemicals

The concentration of experimental solutions was prepared by dissolving a defined amount of salt in fresh pure water (ultrapure water type I with a resistivity of 18.2 M Ω -cm, Purelab Ultra, ELGA). NO_3^- salts, potassium nitrate (KNO_3), sodium nitrate (NaNO_3), calcium nitrate ($\text{Ca}(\text{NO}_3)_2$), magnesium nitrate ($\text{Mg}(\text{NO}_3)_2$), and sodium sulfate (Na_2SO_4),

Table 1
Characteristics of the commercial membranes

Characteristics	NF 90	NF270	UF
ΔP_{\max}	41 [19]	41 [19]	100
Surface area (cm ²)	138	138	24.5
Pore size (nm)	0.55–0.13 [20]	0.71–0.14 [20]	5
pH range	3–10 [19]	3–10 [19]	1–14
<i>T</i> (°C) maximum	45 [19]	45 [19]	95
MWCO (Da)	200 [19]	300 [19]	-
Isoelectric point IEP (KCl 10 ⁻³ M)	4 [19]	2.9–3 [19]	8–9 [5]
Zeta potentiel (mV) (1 mM KCl for NF and 1 mM NaCl)	From 23 to 9 mV for pH (from 2 to 4) [22]	From 12 mV for pH (from 1 to 2.5) [22]	From 31.3 to 37.0 mV for pH (from 1 to 7.5) [23]
	From -3 to -39 mV for pH (from 4.7 to 10.5) [22]	From -5 to -62 mV for pH (from 3.5 to 10) [22]	From -35.3 to -36.5 mV for pH (from 9 to 12) [23]
Charge (neutral pH)	Negative [19]	Negative [19]	Positive
Material	Polyamide [19]	Polyamide [19]	Gamma alumina

besides, solvent and reagents used in the course of experiments were of analytical grade with high purity and acquired from Sigma-Aldrich (Darmstadt, Germany).

2.2. Measurement and analytical techniques

2.2.1. Contact angle measurements

To investigate the hydrophobicity/hydrophilicity of the studied membranes, the contact angle (CA) between pure water and membranes' surfaces was measured according to the sessile-drop method using a goniometer (DGD-MCAT, France). Prior to examination, membrane samples were firstly rinsed with deionized water and dried in a silica gel desiccator (at 23°C). Afterward, droplets (a drop of about 10.0 μ L and pH 6.6) of pure water were deposited on the flat homogeneous membranes' surface and a static image of the droplets in equilibration with the membrane surface were taken. The CA of each droplet was measured at the steady-state 30 s. Reported values are the average CA of droplets deposited on various places upon the membrane's surface. The membrane's surface is hydrophilic when the CA angle θ is <90° and hydrophobic when CA θ is >90°.

2.2.2. Analytical methods

The concentration of ions in the permeate samples, obtained from the various synthetic solutions, was determined by means of diverse measurement techniques. All synthetic samples and NO₃⁻ feed solutions (binary and ternary solutions) for filtration and analysis were prepared by appropriate dilution of the stock solution. NO₃⁻ concentration was colorimetrically determined at a wavelength of 415 nm by UV-vis spectrophotometer (UNICAM UV2 UV/vis spectrometer, ATi), following the international organization for standardization (ISO78903). SO₄²⁻ ion was determined spectrophotometrically via anion exchange reaction with soluble barium salt at a wavelength of 650 nm. The concentration of Ca²⁺ and Mg²⁺ was analyzed by complexometric titration using EDTA as recommended by the French standard (Afnor-NF/T90-016 and NF/T90-003). The limit

of detection of both cations corresponds to 0.05 mmol/L. Potassium (K⁺) and sodium (Na⁺) concentrations were measured by flame photometer model PFP7 with a limit of detection of 0.2 mg/L. Underground water composition, before and after filtration, was determined via ICP spectrometer (Thermo Scientific iCAP 7000 series ICP-OES, Waltham, MA USA). Triplicate analyses were carried out on each sample and the average concentrations were recorded. pH measurements were carried out with a pH meter-seven compact (Mettler-Toledo GmbH, Analytical, Versailles, France), with an accuracy of ± 0.05 .

2.3. Membranes filtrations experiments

2.3.1. Filtration setup

The membranes' performance was determined using tangential filtration units. The cross-flow pilot used for NF is a stainless steel planar module provided by GE osmonics, with a surface area of 138 cm². The pilot is equipped with a pump HP (Wanner, USA) that includes a feeding circulation speed regulator, a feed tank of 5 L, and a thermostat for setting the desired temperature (fixed at 20°C). It has two valves, one for bypassing the flow of feed and the second valve installed at the outlet of the concentrate for fixing the transmembrane pressure (TMP). To regulate the conversion rate, a flow meter is placed at the outlet of the concentrate. While the cross-flow pilot used for UF is a laboratory-scale filtration pilot made from stainless steel with a tubular membrane module [5,27]. The pilot is equipped with a circulation pump and a feed tank of 3 L with a cooling system to maintain the feed solution temperature at a constant value of 20°. The ΔP was adjusted by means of a compressed gas cylinder (helium). The concentration of feed solution, in both UF and NF experiments, was maintained by recycling both permeate and concentrate to the feed. Schematics of the two filtration pilots are shown in Fig. 2.

Membranes were firstly compacted with deionized water for 30 min, and thereafter, with the studied solutions over 90 min at a fixed TMP of 6 bar. The ΔP varied from 4 to 10 bar and 2 to 6 bar, respectively, for NF and UF experiments.

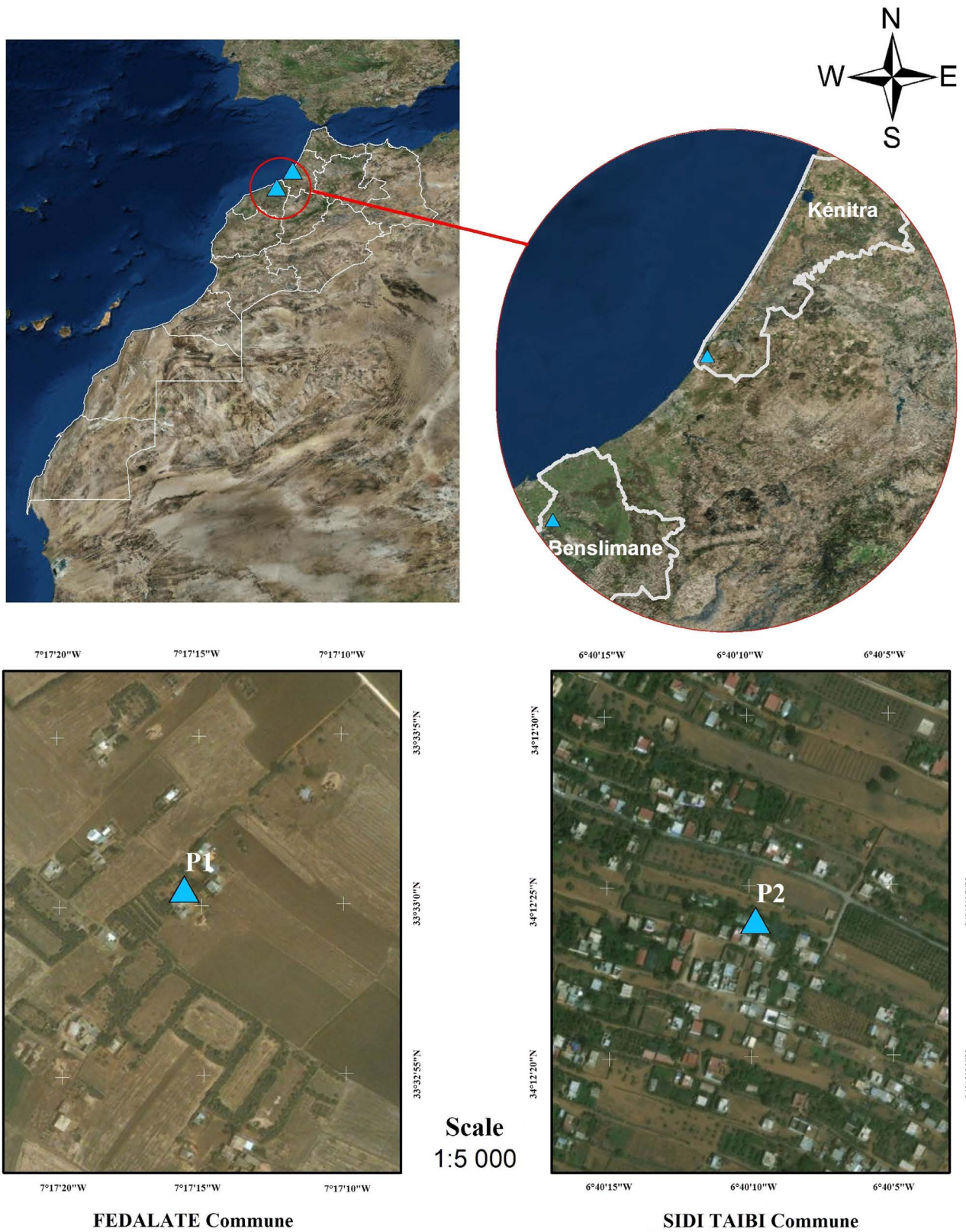


Fig. 1. Geographical setting of the distinct study areas.

Table 2
Characteristics of Moroccan's underground water

Parameters (mg/L)	Commune of Fedalate	Commune of Sidi Taibi	Moroccan standards	WHO guidelines
pH	7.18	6.90	6.0–9.2	6.5–8.5
Ca ²⁺	85.00	103.67	<500	<200
Mg ²⁺	31.47	34.25	<100	<50
Na ⁺	16.57	53.30	<200	<200
K ⁺	2.54	6.69	N.G	N.G
P	<0.20	<0.20		N.G
NH ₄	<0.40	<0.40	0.5	N.G
SO ₄ ²⁻	150	17.00	<200	<250
NO ₃ ⁻	65.74	72.96	<50	<50
Cl ⁻	130.00	57.33	350–750	<250
THT	<0.40	<0.40		
Cu ²⁺	12.00	7.00	2.00	2.00
Zn	5.00	2.00	5.00	3.00
Fe	<0.4	<0.40	0.7–1.5	<0.3
Mn	<0.4	<0.40	0.10	0.50
B	<0.4	<0.40	0.30	0.30
Cr	<0.1	<0.10	0.05	0.05

During filtration, six permeate samples were collected and analyzed. The membranes' reproductively for each experiment were evaluated by three tests, and the values giving in this work are the average. In order to maintain the membranes' initial performance and to remove impurities, a washing of membranes (with deionized water) was done after each experiment. The performance of the membranes was identified by two major parameters that are the rejection rate R (%) and the permeate flux (J_p) (L/h m²), respectively defined by Eqs. (1) and (2):

$$J_p = \frac{V}{A \cdot t} \quad (1)$$

$$R = \left(\frac{1 - C_f}{C_i} \right) \times 100 \quad (2)$$

where C_f , C_i (mg/L), and V (L) are, respectively, the permeate concentration, feed concentration, and the volume of permeate collected during a time interval t (h) according to membrane's effective area A (m²).

Given the major influence of feed rate (that is the conversion or recovery rate (Y)) on ions rejections [25,26], Y was calculated and maintained at a relatively low level for all experiments. Y (%) is defined based on the feed rate (Q_0) and the permeate flow rate (Q_p) as follows:

$$Y = \left(\frac{Q_p}{Q_0} \right) \times 100 \quad (3)$$

2.3.2. Operating procedure

The performance of each membrane in treating NO₃⁻ salts solutions, with different complexity, was carried out

in three consecutive steps. Firstly, membranes' wettability and permeability were characterized. The variation of multiple parameters (pH, pressure, initial NO₃⁻ concentration, and the influence of co and counter-ions) on NO₃⁻ rejection (and its associated cation) was the objective of the second step (as illustrated in Table 3). The effect of pH on J_p of NaNO₃ salt and NO₃⁻ rejection was studied in the pH range 2–9, at a fixed concentration of 50 mg(NO₃⁻)/L, $Y = 5\%$, and $\Delta P = 6$ bar. The effect of pressure and the influence of the associated cation on NO₃⁻ rejection by NF90 and NF270, were simultaneously studied and compared with UF. The ΔP varied from 4 to 10 bar at natural pH (around 5.70–6.50) and concentration of 50 mg(NO₃⁻)/L for single salt with monovalent cation (NaNO₃ and KNO₃), divalent cations (Ca(NO₃)₂ and Mg(NO₃)₂) and for the mixed solution (Mg(NO₃)₂ + Ca(NO₃)₂).

The effect of NO₃⁻ concentration was investigated in the range of 25–100 mg(NO₃⁻)/L. This study was done on solutions with single salts (NaNO₃ and Ca(NO₃)₂) and mixed salts (Ca(NO₃)₂+NaNO₃), at a natural pH, $\Delta P = 6$ bar for UF, and $\Delta P = 10$ bar for NF membranes. Furthermore, to study the influence of co-ions, the molar ratios SO₄²⁻/NO₃⁻ was fixed at 1/1, 2/1, and 3/1 (being sodium the counter-ion) at natural pH and $\Delta P = 6$ bar. Finally, the three membranes were used for underground water denitrification at a pressure of 6 bar and natural pH (6–7). The characteristics of the studied ions are presented in Table 4.

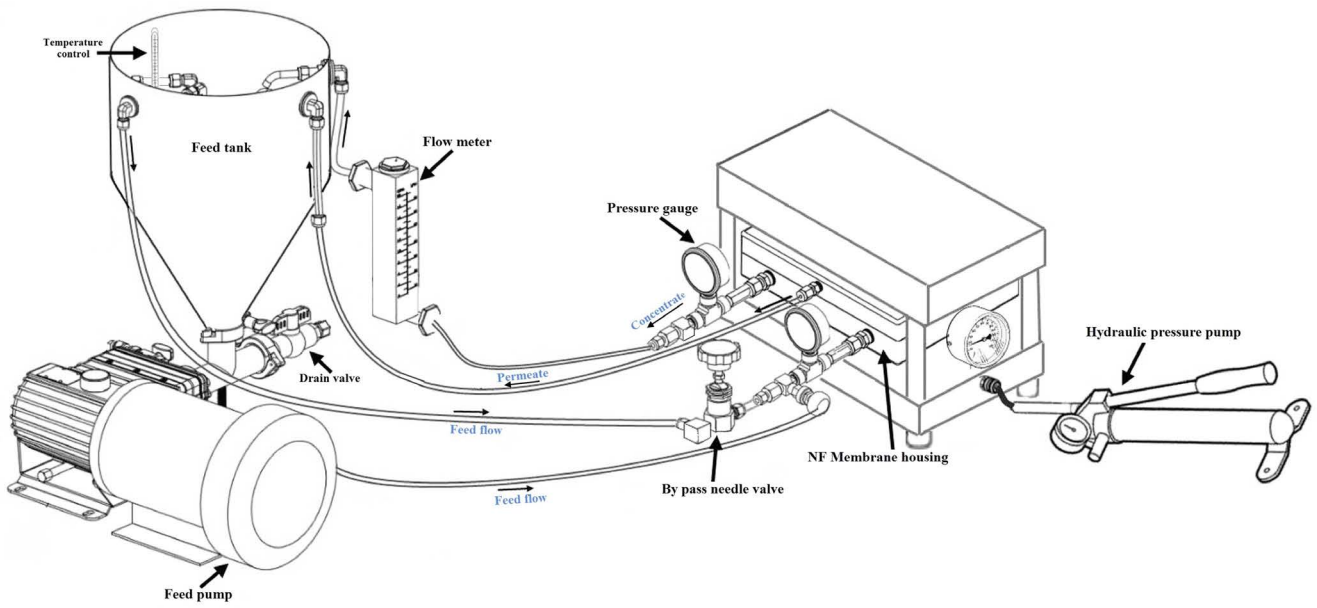
3. Results and discussion

3.1. Membrane characterization

3.1.1. CA measurements

The images in Fig. 3, represent the results of CA measurements of the three membranes using the drop method with pure water. The CA of the studied membranes

(a)



(b)

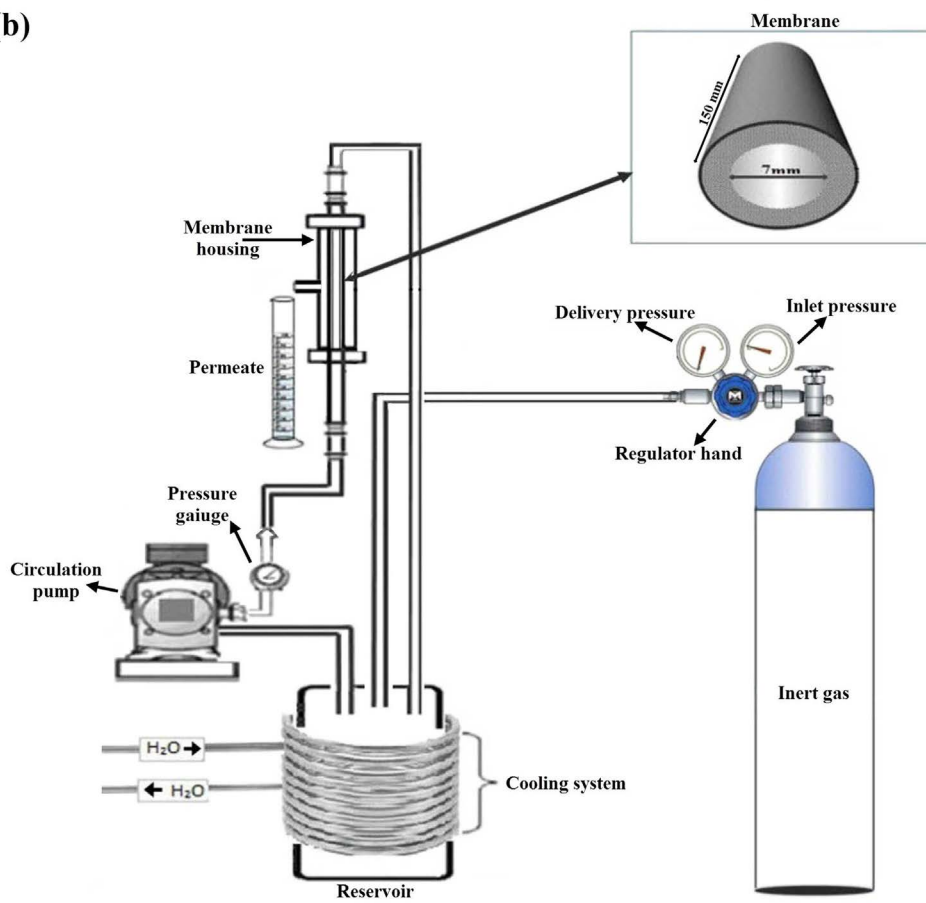


Fig. 2. Schematic illustration of NF pilot (a) and UF pilot (b) [5].

Table 3
Experiments' summary

pH effect on membranes' performance												
Salt	Feed concentration (mg/L)	ΔP (bar)	γ (%)	Temperature (°)	Time (min)	pH	R(%) by NF90	R(%) by NF270	R(%) by γ -Al ₂ O ₃	Flux of NF90	Flux of NF270	Flux of γ -Al ₂ O ₃
NaNO ₃	50	6	5	20	90	2 ± 0.5						
						3 ± 0.5						
						4 ± 0.5						
						5 ± 0.5						
						6 ± 0.5						
						7 ± 0.5						
8 ± 0.5												
9 ± 0.5												
Pressure effect on membranes' performance												
Single Salt	Feed concentration (mg/L)	pH	γ (%)	Temperature (°)	Time (min)	ΔP (bar)	R(%) by NF90	R(%) by NF270	R(%) by γ -Al ₂ O ₃	Flux of NF90	Flux of NF270	Flux of γ -Al ₂ O ₃
KNO ₃ NaNO ₃ Mg(NO ₃) ₂ Ca(NO ₃) ₂	50	5–6	5	20	90	4 ± 0.2						
						5 ± 0.2						
						6 ± 0.2						
						8 ± 0.2						
10 ± 0.2												
Mixed Salt	Feed concentration (mg/L)	ΔP (bar)	γ (%)	Temperature (°)	Time (min)	ΔP (bar)	R(%) by NF90	R(%) by NF270	R(%) by γ -Al ₂ O ₃	Flux of NF90	Flux of NF270	Flux of γ -Al ₂ O ₃
Mg(NO ₃) ₂ + Ca(NO ₃) ₂	50	5–6	5	20	90	4 ± 0.2						
						5 ± 0.2						
						6 ± 0.2						
Concentration effect on membranes' performance												
Salt	ΔP (bar)	γ (%)	pH	Temperature (°)	Time (min)	Feed concentration (mg/L)	R(%) by NF90	R(%) by NF270	R(%) by γ -Al ₂ O ₃	Flux of NF90	Flux of NF270	Flux of γ -Al ₂ O ₃
NaNO ₃ Ca(NO ₂) ₃ NaNO ₃ + Ca(NO ₃) ₂	10 bar for NF, 6 bar for UF	10	5–6	20	90	25						
						50						
						75						
100												
Salt	ΔP (bar)	γ (%)	pH	Temperature (°)	Time (min)	Feed concentration (mg/L)	R(%) by NF90	R(%) by NF270	R(%) by γ -Al ₂ O ₃	Flux of NF90	Flux of NF270	Flux of γ -Al ₂ O ₃
NaNO ₃ + Na ₂ SO ₄	10 bar for NF, 6 bar for UF	10	5–6	20	90	1 (SO ₄ ²⁻)/1(NO ₃ ⁻)						
						2 (SO ₄ ²⁻)/1(NO ₃ ⁻)						
						3 (SO ₄ ²⁻)/1(NO ₃ ⁻)						

Table 4
Properties of related cations and anions

Ion	Ionic weight (Da)	Ionic radius (nm)	Hydrated radius (nm)	Hydrated energy (Kg/mol)	Diffusivity (10^{-9} m ² /s)
Na ⁺	23.0	0.117	0.358	−405	1.334
Mg ²⁺	24.3	0.072	0.428	−1,922	0.706
Ca ²⁺	40.0	0.100	0.412	−1,592	0.792
Cl [−]	35.5	0.194	0.332	−363	2.032
SO ₄ ^{2−}	96.0	0.290	0.379	−1,145	1.065
K ⁺	39.0	0.149	0.331	−321	1.957
NO ₃ [−]	63.0	0.189	0.340	−328	1.902

References [5,29,57]

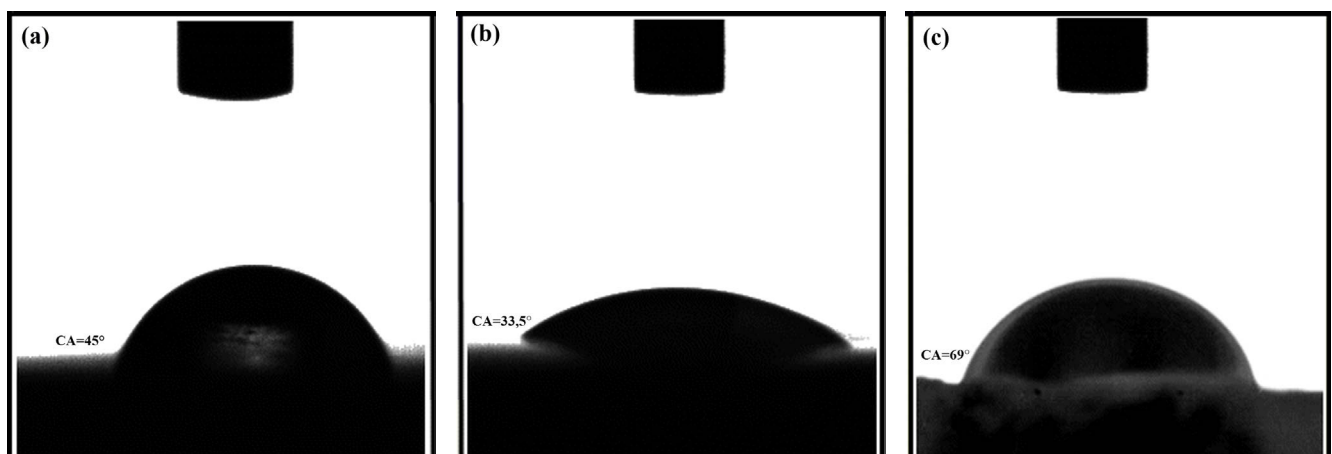


Fig. 3. CA of pure water with the surface of the studied membranes (a) NF90, (b) NF270, and (c) UF.

(UF and NF) was lower than 90°C. With $CA_{(UF)} = 63^\circ > CA_{(NF90)} = 45^\circ > CA_{(NF270)} = 33.5^\circ$, demonstrating a hydrophilic surface.

The hydrophilic character of the NF polyamide membranes is mainly associated with the existence of carboxylic and amine functional groups capable of interacting with water molecules by hydrogen bonds [28,29]. The polyamide layer of NF270, is characterized by lower surface roughness, more linear hydrophilic structure with carboxyl groups, and higher permeability than NF90, resulting in a lower CA [30]. It should be noted that CA does not directly affect the salt rejection; however, it can help in determining the transport of water across the membrane which strongly impacts the overall rejection of a membrane [31]. The surface roughness of membranes is considered one of the main factors responsible for the difference found for the measured CA [32].

3.1.2. Membranes permeability

The hydraulic permeability (L_w) of UF and NF membranes was measured with pure water under different operating pressure, using Eq. (1). In Fig. 4, the interval and mean values of flow measures for the three membranes are plotted.

A clear distinction was observed between L_w of inorganic γ -Al₂O₃ UF membrane and that of the two organic NF membranes. The membranes' permeability was found to be equal 3.93 and 4.60 L/h m² bar for NF90 and NF270, respectively, whereas a value of 5.03 L/h m² bar was recorded for γ -Al₂O₃ UF membrane. The difference in NF membranes' permeability is in good correlation with the results obtained for CA of NF. NF Membrane with high CA has the lowest permeability. γ -Al₂O₃ UF membrane is more permeable than the NF membranes due to a difference in pore diameter. UF has the highest pore size and high porosity, and thus high water permeability. In general, the pore size gives a better correlation than CA, this latter is affected by the membrane's roughness, pore size distribution, and shape [33,34].

3.2. Influence of operating parameters on NO₃[−] removal

3.2.1. Influence of solution pH

3.2.1.1. Influence of solution pH on J_p

The ions' separation is governed by the active charge of the surface layer of membrane (UF or NF) which differs according to membrane's material and solution's pH [35,36].

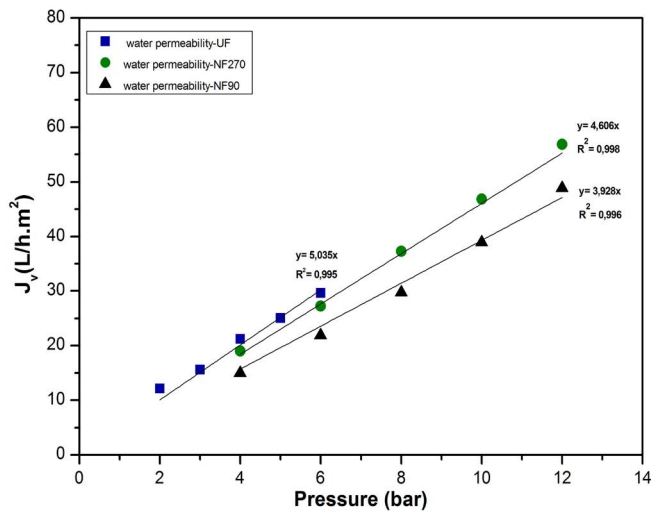


Fig. 4. Pure water flux as a function of ΔP for NF and UF membranes ($T = 20^\circ\text{C}$ and $\text{pH} = 6.5$).

The studied membranes are characterized by amphoteric behavior.

NF amphoteric character is related to the presence of various functional groups on the membrane surface. At pH values above pH_{IEP} (pH at the iso-electric point (IEP)), the membrane is negatively charged resulting from a high degree of deprotonation of the carboxylic functional groups ($\text{R}-\text{COO}^-$). While the positive charge at low pH values is attributed to the protonation of the amine functional groups ($\text{R}-\text{NH}_3^+$). The UF amphoteric character is demonstrated by the negative surface charge at $\text{pH} > \text{pH}_{\text{IEP}}$ attributed to the acidic dissociation of the surface hydroxyl groups (AlO^- groups). The positive charge at $\text{pH} < \text{pH}_{\text{IEP}}$ is explained by proton addition to the neutral aquo-complex (AlOH_2^+ groups) [37].

Fig. 5a, presents the J_p of the three membranes as a function of pH (2.5–9.5) at a fixed NO_3^- concentration of 50 mg/L and ΔP of 6 bar. The pH variation had no significant effect on salt permeability. For both NF90 and NF270 membranes, the flux increased slightly with pH increase until reaching a maximum close to the IEP (around pH 3–4). The flux decreased marginally at near to membranes' IEP and remained constant as the pH increases beyond IEP. Similar results were found by other authors [37,38]. For the UF membrane, the flux was found to slightly decrease with increasing pH until a value of 7.2, which was near the membrane IEP. When pH is higher than pH_{IEP} the J_p increases with pH. Similar findings have been reported with $\alpha\text{-Al}_2\text{O}_3$ and $\gamma\text{-Al}_2\text{O}_3$ membranes [5,27,39]. The NF membrane skin could swell with an increase of pH, which results in a lower filtration resistance [40]. At the same time, the electrical charge of NF membranes rose with pH and stronger NO_3^- repulsion will happen, resulting in higher osmotic pressure (a loss in driving force). These opposite parameters cause an insignificant change in the water permeability of membranes. We suppose that the surface interaction of UF membrane is more pronounced than NF membrane which may explain the flow reduction [41]. Further, the presence

of electrolytes in solution contributes to an extra resistance to the flux transfer across the membrane.

To summarize, the pH effect on salt flux is not marked, and this for all membranes (J_v (acid) = J_v (neuter) = J_v (basic)). Fluxes were nearly constant for all membranes (between 19 and 22 L/h m²).

To better understand the main mechanisms governing the J_p , Childress and Elimelech [42], proposed mechanisms relating the change of pore size with pH variation as follow:

- The expanding or shrinking of the cross linked-membrane network;
- The electroviscous effect;
- The highest net driving force due to the lowest osmotic pressure at the membrane surface.

3.2.1.2. Influence of solution pH on NO_3^- rejection

Fig. 5b, illustrates the influence of pH on the retention of NO_3^- ions during the filtration of NaNO_3 ($\text{Ci} = 50 \text{ mg}(\text{NO}_3^-)/\text{L}$) (at $\Delta P = 6$ bar, $Y = 5\%$, and $T = 20^\circ\text{C}$). It is found that the increase in pH has caused a significant increase in the retention of NO_3^- (for both NF membranes). At $\text{pH} < \text{pH}_{\text{IEP}}$ the NF membrane is positive, therefore, NO_3^- ions would permeate more easily into the membrane resulting in a decrease of rejection (NO_3^- rate rejection at pH 3 for NF90 and NF270 are, respectively, 41% and 33%). However, increasing the solution pH led to an increase in the negative charge density of NF membranes. This growth of charge enhances electrostatic repulsion with anions. Consequently, the retention of NO_3^- would be higher because of charge repulsion [43] and sieving mechanism especially in case of NF90 (at pH 8, the rejections are in the order of 70% and 41% for NF90 and NF270, respectively). For $\gamma\text{-Al}_2\text{O}_3$ UF membrane, the NO_3^- rejection (of 50%) also increased when pH increase (from pH 2 to 7). This increase of rejection is explained by the high cation repulsion (as both membrane surface and cations are positively charged) which leads to NO_3^- retention due to electroneutrality consideration. The decrease in retention, at pH_{IEP} is caused by a dominance of the sieving mechanism. For $\text{pH} > \text{pH}_{\text{IEP}}$, although both membrane and NO_3^- are negatively charged a decrease in salt retention was observed. This decrease was explained by a reduction in the positive charge of $\gamma\text{-Al}_2\text{O}_3$ membrane and thus the electroneutrality mechanism. In fact, at pH above 9, the membrane is negatively charged which facilitates the passage of cations through the membrane to the permeate side. Under the dominance of size effect and according to Donnan equilibrium, NO_3^- will follow the cation's passage [5,44]. The better rejection obtained for UF compared to NF 270, can be explained by the difference of surface charge which dramatically affects the electroneutrality's balance and NO_3^- rejection. The greater surface charge of UF membrane and thus the stronger electrostatic repulsive force against NO_3^- explain the obtained results [45]. In summary, good rejections of NO_3^- by NF90 and $\gamma\text{-Al}_2\text{O}_3$ UF were obtained at $\text{pH} \geq 5$, and $\text{pH} = 7$, respectively. The Donnan effect is of significant importance in membranes when treating an electrolyte solution [46], especially for UF membrane. The size effect is also dominant in the case of NF90.

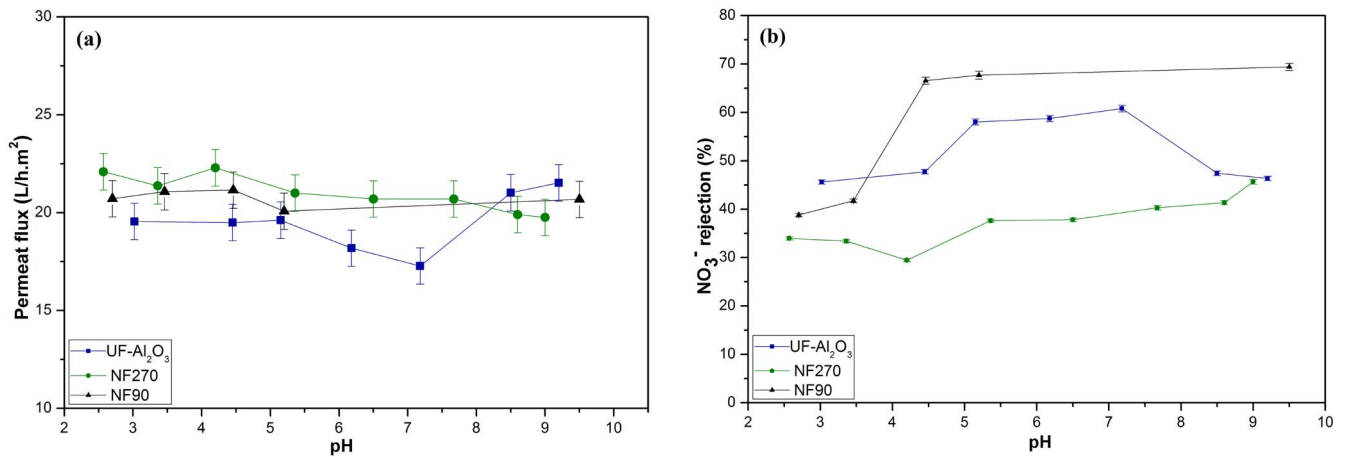


Fig. 5. Influence of feed pH on permeate flux of NaNO₃ solution (a) and NO₃⁻ rejection (%) and (b) (at fixed ΔP and C_i of 6 bar and 50 mg(NO₃)/L, respectively, $Y = 5\%$, and $T = 20^\circ\text{C}$).

3.2.2. Influence of applied pressure (ΔP) on NO₃⁻ rejection

The results of the effect of pressure performed on NF membranes were compared with UF membrane's results, as illustrated in Fig. 6. From Fig. 6a, the increase of pressure has resulted in rejection increase and this for the three membranes. The rejection of NO₃⁻ relies on the solute concentrations in permeate and at the membrane surface, due to the combined results of convection and diffusion mechanisms [47]. The convection has a direct effect on NO₃⁻ retention at high pressure, while, the diffusion plays a major role at low pressure leading to a decrease of salt retention (especially salt with monovalent cation) [48]. In fact, the solvent could pass through the membrane by convection, while NO₃⁻ rejection would rely on solute concentrations in permeate and at the membrane surface. NF90 membrane shows the highest NO₃⁻ rejection among the other membranes. This finding can be explained by the membrane's smaller pore size as well as the electrostatic repulsion between the membrane negative charge and NO₃⁻. NF90 is found to be close to RO than NF membranes, therefore the size effect plays an important role and explains the high obtained retentions [49,50]. Furthermore, the high surface roughness of NF90 enhances NO₃⁻ rejection. NF270 membrane has a relatively larger pore diameter, hence very low rejections [51,52]. The high retentions obtained by UF compared to NF270, are mainly due to electroneutrality consideration. In fact, the difference of surface charge (at the studied pH) of NF270 (negative charge) and UF (positive charge) plays a crucial role in the electroneutrality principle. For NF270, the co-ion (in our case NO₃⁻) is moderately rejected outside the membrane by repulsion. In order to ensure the electroneutrality's balance on both sides of the membrane, cations are also rejected. The NF270 counter-ions (cations, Ca²⁺, Mg²⁺, Na⁺, and K⁺) screen progressively the membrane charges, and thus the NO₃⁻ ions pass across the membrane. The difference in salts' rejection (for the three membrane) depends on the ionic species' charge and that of the membrane. The rejection of NO₃⁻ varies according to the associated cation, and increases in the following order: K⁺ < Na⁺ < Ca²⁺ < Mg²⁺ respecting the Donnan equilibrium. Salt with the cation of

lowest diffusivity and highest hydrated radius is the best retained. In UF filtration, the Donnan effect plays a very important role that cannot be ignored [5,24].

3.2.2.1. Influence of applied pressure (ΔP) on NO₃⁻ rejection for mixed salt

Fig. 6b, demonstrates the results obtained for mixed salts (Mg(NO₃)₂+Ca(NO₃)₂) at natural pH and concentration of 50 mg(NO₃)/L, under the influence of ΔP . The same behavior (an increase of NO₃⁻ rejection with pressure) was observed for mixed salt. NF90 allows strongly reducing the concentration of NO₃⁻. The rejections obtained for the three membranes are not in the same order (RNF90 (%) > RUF (%) > RNF270 (%)). Moreover, the rejection of mixed salts was weakly found to be lower than the rejection of the two salts treated separately (Mg(NO₃)₂ and Ca(NO₃)₂). The charge of the associated cation (divalent one, Mg²⁺, and Ca²⁺) and membrane surface affect the rejection of NO₃⁻. Since the cation with a high hydrated radius (ion's size) and charge density is better rejected by UF and thus NO₃⁻. Generally, the existence of different charge groups (positive/negative) on the membrane surface leads to an increase in the electrostatic interaction phenomenon widely known by counter-ion site binding [53].

3.2.3. Influence of NO₃⁻ concentration on NO₃⁻ rejection

3.2.3.1. Influence of the counter-ion concentration on the retention of NO₃⁻

The influence of salt concentration on NO₃⁻ rejection is a critical parameter to study, for the three membranes. The results of UF filtration used in this study are those obtained in our first article [5]. The experiments were performed with different NO₃⁻ solutions at natural pH (5–6), $Y = 10\%$, $T = 20^\circ\text{C}$, and fixed ΔP of 6 and 10 bar respectively for UF and NF membranes.

As shown in Fig. 7, the increase of NO₃⁻ concentration contributed to a decrease in NO₃⁻ rejections, and this for the three membranes and different solutions. The high

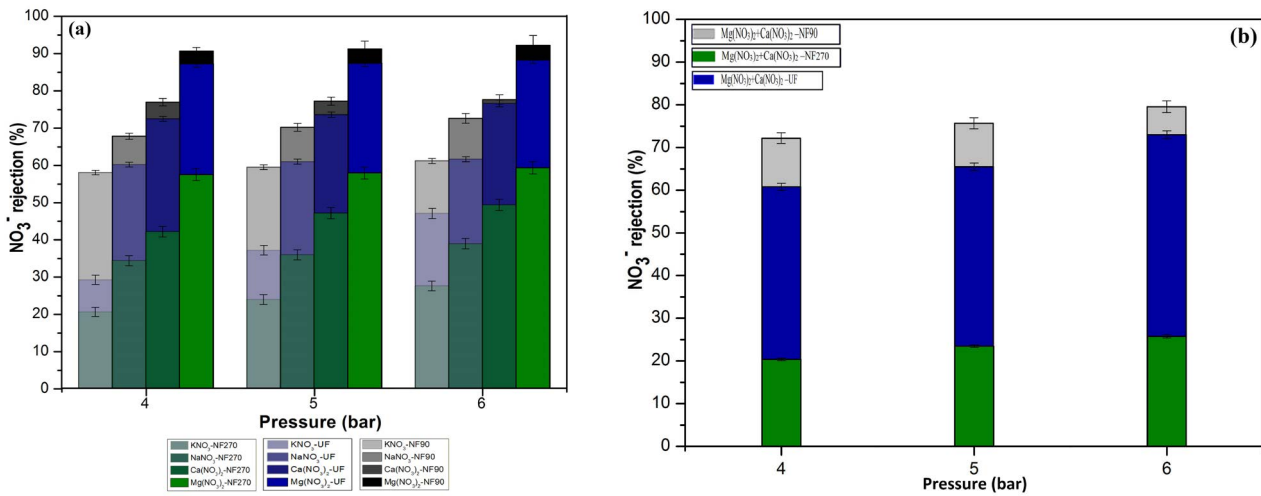


Fig. 6. Comparative study on the effect of pressure on NO₃⁻ rejection by NF90, NF270, and γ -Al₂O₃ UF membrane for single salts (a) and mixed salts (b) (for 90 min of filtration, at a fixed concentration $C_i = 50 \text{ mg}(\text{NO}_3^-)/\text{L}$, $Y = 5\%$, $T = 20^\circ\text{C}$, and natural pH (5–6)).

rejections were obtained for NF90 membrane (rejection exceeded 80% independently of the NO₃⁻ feed concentration) followed by the rejections achieved by UF membrane (80% is the highest value obtained for Ca(NO₃)₂ at $C_i = 25 \text{ mg}(\text{NO}_3^-)/\text{L}$, the lowest value was equal to 44% for mixed salt at $C_i = 100 \text{ mg}(\text{NO}_3^-)/\text{L}$) and then NF270 (the highest rejection was found at $C_i = 25 \text{ mg}(\text{NO}_3^-)/\text{L}$ with a value of 60% for Ca(NO₃)₂, and the lowest value was of 55% at $C_i = 100 \text{ mg}(\text{NO}_3^-)/\text{L}$). This decrease of rejection with increasing concentration is mainly interpreted by the shielding (screen) phenomena [37,54]. As a matter of fact, the increase in concentration implies the increasing formation (by cation Na⁺, Ca²⁺ in our case) of a screen layer which neutralizes the negative charge of NF membrane and reduces the repulsion force between the NF membrane and NO₃⁻. The decline in NO₃⁻ rejection could also be explained by a difference in concentration between the membranes' two sides (feed and permeate sides). Based on this distinctness of concentration, ion diffusion across the membrane happened [45,55]. Further, the rejection dramatically decreases when the concentration increases for salts with monovalent cation (NaNO₃). While for NF90, NO₃⁻ rejection of salt with divalent cation (Ca(NO₃)₂) did not depend on the concentration (NO₃⁻ rejection exceeded 85% for all concentrations) [43,56]. The low rejections obtained for cations with low charge densities (such as Na⁺) were because of the weak repulsion forces between the membranes and monovalent ions. The high rejection obtained for Ca²⁺ is due to the capacity of NF membrane to maintain the solution's electroneutrality, as well as, the capacity of Ca²⁺ to be adsorbed to the membrane surface [37,57]. For mixed salts (NaNO₃+Ca(NO₃)₂), NO₃⁻ rejection strongly decreases with concentration and remains lower than the results obtained with single salts. The Na⁺ rejections in mixed salts, by NF90, were equal to 73% and 61.6%, respectively for 25 and 100 mg(NO₃)₂/L concentration. While for single salt (NaNO₃), rejections were respectively equal to 75.7% and 65% for 25 and 100 mg(NO₃)₂/L. Similar to single salts, these results could be interpreted by a decrease of the effective charge when the concentration

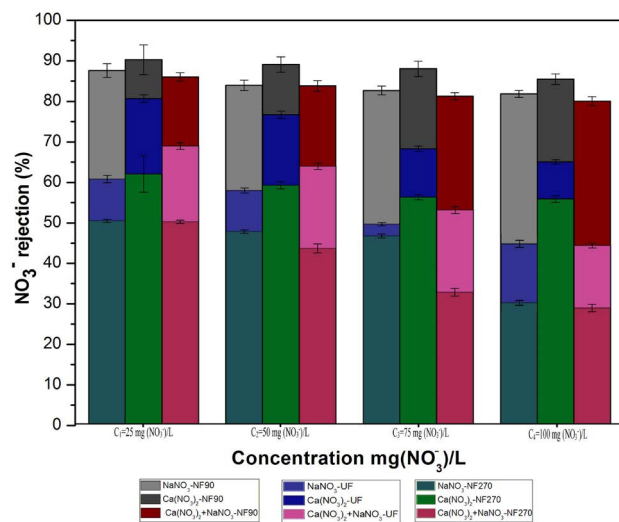


Fig. 7. Comparative study on the effect of NO₃⁻ concentration on the performance of NF90, NF270, and γ -Al₂O₃ UF membranes (for single salts and mixed salts after 90 min of filtration, natural pH (5–6), $Y = 10\%$, $T = 20^\circ\text{C}$, and $\Delta P = 10 \text{ bar}$ for NF and $\Delta P = 6 \text{ bar}$ for UF).

growth. Further, the monovalent cation (Na⁺) passes easily through the membrane compare to Ca²⁺, therefore, a define amount of NO₃⁻ will also pass through the membrane to keep electroneutrality of the membrane solution.

To summarize, the NF90 has the smallest pores size among NF270 and UF and thus the retention was higher because of the size and charge effects [54]. Giving the relatively high pressure and conversion rate, the low NO₃⁻ rejections obtained by NF270 were attributed to the compaction of the electrical double layer of the membrane surface and the size effect [58]. According to Nilsson et al. [59], Lyotropic effects (also called salting effect) can be expected in the presence of high salts. The association of macromolecular structure in the presence of high

salt concentration decreases the electrolyte solubility and reduces NO_3^- rejection. Another explanation, based on the membranes' pore size distribution, is that the increase of salt concentration reduces the flux of small pores to a higher extent than larger pores leading to a decrease in solute retention [60]. For NF90, the constant rejection (mostly high) at high NO_3^- concentrations is attributed to the importance of membrane–solute electrostatic interactions that remain constant even at high concentration and also to the pore size [56].

3.2.3.2. Influence of the co-ion concentration on the retention of NO_3^- in a binary mixture

The previous studies established the critical effect of the hydration energy of cations and its valence on NO_3^- retention with the three membranes. To study the influence of co-ions on the retention of NaNO_3 salt, experiments were performed by varying the molar ratio of SO_4^{2-} (as NO_3^- co-ion) in the mixed salts solution ($\text{NaNO}_3 + \text{Na}_2\text{SO}_4$). Fig. 8, illustrates the rejection results obtained for the ternary system $\text{NO}_3^-/\text{SO}_4^{2-}/\text{Na}^+$ after 90 min of filtration at natural pH, $\Delta P = 6$, and $T = 20^\circ\text{C}$. The NO_3^- concentration was fixed at 100 mg/L.

As can be seen in Fig. 8, the retention of both anions is not in the same order. A significant decrease in NO_3^- rejection was obtained with an increase of SO_4^{2-} concentration. Additionally, the retentions of SO_4^{2-} were considerably high (e.g., the solution with a molar ratio of $\text{SO}_4^{2-}/\text{NO}_3^- = 1$, have rejections $> 90\%$ and $> 50\%$, respectively for NF90 and UF) even with the increase of the added Na^+ . The presence of high valence anions leads to a high level of NO_3^- in the membranes which could reduce its rejection [43,56]. As a matter of fact, the significant SO_4^{2-} rejection forced NO_3^- ions to pass through the membranes to counterbalance the transfer of Na^+ ions (Na^+ rejections were found to be 89% and 6%, respectively, for NF90 and UF). The high rejection of SO_4^{2-} (rate rejection above 90%) by NF90, might be explained by its divalent charge and/or to their size. Indeed, the force of electrostatic repulsion with the membrane is profoundly strong because of the divalent charge of anion.

3.2.4. Denitrification of Moroccan groundwater

Fig. 9 presents the results of the evaluation and comparison of the performance of the three membranes in water denitrification of the Moroccan agricultural areas. The experiments were done at different pressure (ΔP (4–6) and at natural pH (6–7)).

As regards to groundwater's denitrification and membrane type, a considerable difference was noticed in accordance with the degree of mineralization of the two water (Table 2). As illustrated in Fig. 9, the highest NO_3^- rejections (of 64% and 56%, respectively, for NF90 and $\gamma\text{-Al}_2\text{O}_3$ UF) were obtained at 6 bar for Sidi Taibi groundwater compare to the other agricultural area.

NF90 membrane demonstrated the best rejection and this for all ions, (illustrated in Table 5). Additionally, the UF membrane showed a better NO_3^- rejection than NF270. The weak rejection obtained in Fedalate water is explained by the high presence of anions in particular SO_4^{2-} and Cl^- (Table 2). This result confirms the obtained conclusions on the studies of NO_3^- behavior in mixture solution, which

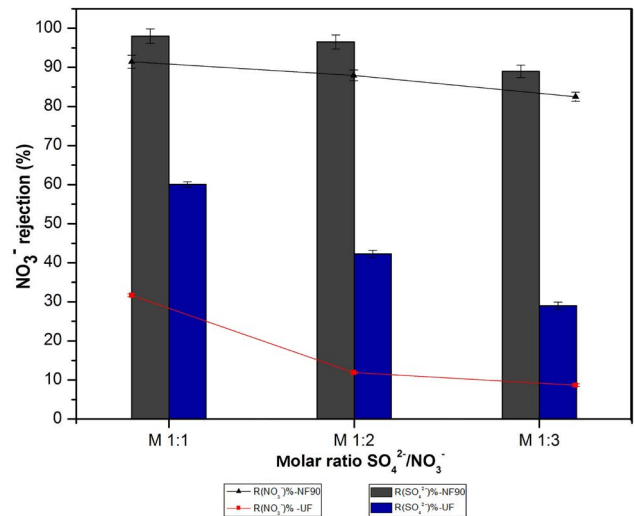


Fig. 8. Ionic rejection vs. molar ratio $\text{SO}_4^{2-}/\text{NO}_3^-$ for the ionic system $\text{NO}_3^-/\text{SO}_4^{2-}/\text{Na}^+$ as a function of NO_3^- ion concentration at natural pH ($\Delta P = 6$, $Y = 5\%$, and $T = 20^\circ\text{C}$).

resulted in a decrease of NO_3^- rejection when the complexity of the solution is very high and when the presence of anions is big. Indeed, the rejections of SO_4^{2-} by NF90, UF, and NF270 membranes were, respectively, in the order of, 86%, 67%, and 65% for Sidi Taibi groundwater, while rejections of 51%, 27%, and 19% were found for Jamaat Fedalate groundwater. Based on this finding, the NF90 membrane can be used for partial denitrification of contaminated water especially in agricultural Moroccan areas. The $\gamma\text{-Al}_2\text{O}_3$ UF membrane showed good potential in NO_3^- removal than NF270. This finding is explained by the electrostatic repulsion of cation caused by the positive charge of the membrane at natural pH for UF membrane. While the cation is rejected, the anion (NO_3^-) is retained to keep solution electro-neutrality, which answers the Donnan equilibrium.

4. Conclusion

To confirm the suitability of inorganic UF membranes in NO_3^- removal, a comparative study was made on three commercial membranes (NF90, NF270, and $\gamma\text{-Al}_2\text{O}_3$ UF) using model water solutions (binary and ternary solutions) and contaminated underground water (of two distinct regions).

The results showed that NF90 membrane has high rejection (above 80% for single salt) while UF demonstrated a better NO_3^- rejection than NF270. For the NF 90 membrane, the transfer mechanism involving sieving and electrostatic interaction effects appear to play an important role. The suitability of UF over NF270 membrane for the removal of NO_3^- ions is caused by the Donnan effect (charge pattern-electroneutrality). Parameters such as solute hydration energy, membrane-solute interaction, and solute-solute interaction were found to be of great influence.

The selectivity of the three membranes strictly depended upon the feed pH, ΔP , and ion concentration. The increase in pH led to higher NO_3^- rejection due to the increase in the negative charge of NF membrane. For UF membrane, the high rejection of NO_3^- was obtained around pH_{IEP} . The increase

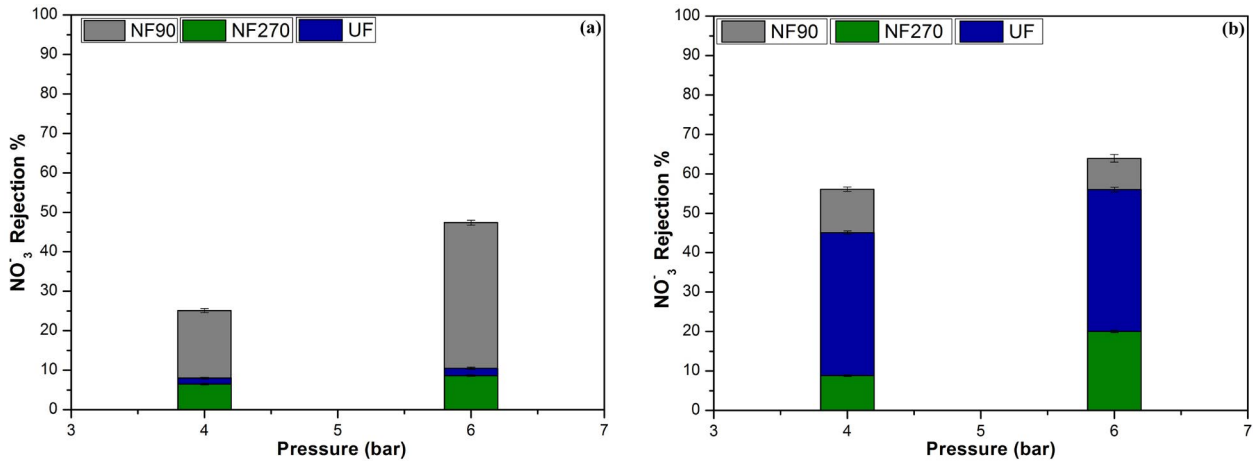


Fig. 9. Comparative study of NO₃⁻ retention (%) as a function of the type of membrane and groundwater (a) Jamaa Fedalat and (b) Sidi Taibi (at natural pH (6–7); $\gamma = 15\%$, $T = 25^\circ\text{C}$, and $\Delta P = 4\text{--}6$).

Table 5
Permeate characterization of Sidi Taibi underground water ($\Delta P = 6$ bar, pH natural)

Underground water	Sidi Taibi		
Membrane type	NF90	NF270	UF
R (Ca ²⁺)%	68.33	20	46.66
R (Mg ²⁺)%	72.99	53.75	62.68
R (Na ⁺)%	80	72.57	53.26
R (K ⁺)%	94.32	95.96	97.31
R (P)%	<0.2	<0.2	<0.2
R (NH ₄ ⁺)%	<0.4	<0.4	<0.4
R (SO ₄ ²⁻)%	86.66	68	65.33
R (NO ₂)%	68.52	46.29	64.81
R (THT)%	<0.4	<0.4	<0.4
R (Zn)%	60	–	55
R (Fe)%	<0.4	<0.4	<0.4
R (Cu ²⁺)%	<0.4	<0.4	<0.4
R (B)%	<0.4	<0.4	<0.4
R (Cr)%	<0.1	<0.1	<0.1

of pressure results in rejection growth while the increase in salt concentration causes a decrease in NO₃⁻ rejection for the three membranes. The increase of divalent anions (e.g., SO₄²⁻) discriminate NO₃⁻ rejection, while, the addition of divalent cations tends to enhance the retention of NO₃⁻. Groundwater with weak total mineralization and weak content in divalent anions, the case of Sidi Taibi groundwater, had the highest value of NO₃⁻ rejection. The obtained results allow considering interesting perspectives for the application of UF in the treatment of NO₃⁻ pollution.

Acknowledgments

The authors wish to acknowledge support from MESRSFC Ministère de l’Enseignement Supérieur et de la Recherche Scientifique et de la Formation des cadres – Morocco) and

CNRST (Centre National pour la Recherche Scientifique et Technique – Morocco) (Project number PPR/2015/72).

References

- [1] A. Naz, B.K. Mishra, S.K. Gupta, Human health risk assessment of chromium in drinking water: a case study of Sukinda chromite mine, Odisha, India, *Exposure Health*, 8 (2016) 253–264.
- [2] M. Breida, S.A. Younssi, M. Ouammou, M. Bouhria, M. Hafsi, Pollution of Water Sources from Agricultural and Industrial Effluents: Special Attention to NO₃⁻, Cr(VI), and Cu(II), M. Eyvaz, E. Yüksel, Eds., *Water Chemistry*, IntechOpen, 2019. Available at: <https://www.intechopen.com/books/water-chemistry/pollution-of-water-sources-from-agricultural-and-industrial-effluents-special-attention-to-no-sub-3->
- [3] S. Jadhav, C. Gadipelly, K. Marathe, V. Rathod, Treatment of fluoride concentrates from membrane unit using salt solutions, *J. Water Process Eng.*, 2 (2014) 31–36.
- [4] B. Bendra, S. Fetouani, X. Laffray, M. Vanclooster, M. Sbaa, L. Aleya, Effects of irrigation on soil physico-chemistry: a case study of the Triffa Plain (Morocco), *Irrig. Drain.*, 61 (2012) 507–519.
- [5] M. Breida, S.A. Younssi, A. Bouazizi, B. Achiou, M. Ouammou, M. El Rhazi, Nitrate removal from aqueous solutions by $\gamma\text{-Al}_2\text{O}_3$ ultrafiltration membranes, *Heliyon*, 4 (2018), doi: 10.1016/j.heliyon.2017.e00498.
- [6] A. Menció, J. Mas-Pla, N. Otero, O. Regàs, M. Boy-Roura, R. Puig, J. Bach, C. Domènech, M. Zamorano, D. Brusi, Nitrate pollution of groundwater; all right... but nothing else?, *Sci. Total Environ.*, 539 (2016) 241–251.
- [7] N.-E. Laftouhi, M. Vanclooster, M. Jalal, O. Witam, M. Aboufirassi, M. Bahir, E.T. Persoons, Pollution par les nitrates des eaux souterraines du bassin d’Essaouira (Maroc), *C.R. Geosci.*, 3 (2003) 307–317.
- [8] S. Fetouani, M. Sbaa, M. Vanclooster, B. Bendra, Assessing ground water quality in the irrigated plain of Triffa (north-east Morocco), *Agric. Water Manage.*, 95 (2008) 133–142.
- [9] F. Mourabit, A. Ouassini, A. Azmani, R. Mueller, Nitrate occurrence in the groundwater of the Loukkos perimeter, *J. Environ. Monit.*, 4 (2002) 127–130.
- [10] M. Gutiérrez, R.N. Biagioni, M.T. Alarcón-Herrera, B.A. Rivas-Lucero, An overview of nitrate sources and operating processes in arid and semiarid aquifer systems, *Sci. Total Environ.*, 624 (2018) 1513–1522.
- [11] Z. Zhang, A. Chen, Simultaneous removal of nitrate and hardness ions from groundwater using electrodeionization, *Sep. Purif. Technol.*, 164 (2016) 107–113.

- [12] G. Hua, M.W. Salo, C.G. Schmit, C.H. Hay, Nitrate and phosphate removal from agricultural subsurface drainage using laboratory woodchip bioreactors and recycled steel byproduct filters, *Water Res.*, 102 (2016) 180–189.
- [13] S.A. Younssi, M. Breida, B. Achiou, Alumina Membranes for Desalination and Water Treatment, M. Eyvaz, E. Yüksel, Eds., Desalination and Water Treatment, InTech, 2018. Available at: <https://www.intechopen.com/books/desalination-and-water-treatment/alumina-membranes-for-desalination-and-water-treatment>
- [14] F.C. Silva, Fouling of Nanofiltration Membranes, M.A. Farrukh, Ed., Nanofiltration, 2018. Available at: <https://www.intechopen.com/books/nanofiltration/fouling-of-nanofiltration-membranes>
- [15] M.A. Abdel-Fatah, Nanofiltration systems and applications in wastewater treatment, *Ain Shams Eng. J.*, 9 (2018) 3077–3092.
- [16] B. Achiou, H. Elomari, A. Bouazizi, A. Karim, M. Ouammou, A. Albizane, J. Bennazha, S.A. Younssi, I. El Amrani, Manufacturing of tubular ceramic microfiltration membrane based on natural pozzolan for pretreatment of seawater desalination, *Desalination*, 419 (2017) 181–187.
- [17] A. Bouazizi, M. Breida, B. Achiou, M. Ouammou, J.I. Calvo, A. Aaddane, S.A. Younssi, Removal of dyes by a new nano-TiO₂ ultrafiltration membrane deposited on low-cost support prepared from natural Moroccan bentonite, *Appl. Clay Sci.*, 149 (2017) 127–135.
- [18] J. Wang, Y. Mo, S. Mahendra, E.M. Hoek, Effects of water chemistry on structure and performance of polyamide composite membranes, *J. Membr. Sci.*, 452 (2014) 415–425.
- [19] H. Dach, Comparison of Nanofiltration and Reverse Osmosis Processes for a Selective Desalination of Brackish Water Feeds, Engineering Sciences [Physics], Université d'Angers, 2008.
- [20] N. Hilal, H. Al-Zoubi, A. Mohammad, N. Darwish, Nanofiltration of highly concentrated salt solutions up to seawater salinity, *Desalination*, 184 (2005) 315–326.
- [21] M. Pontié, C. Diawara, A. Lhassani, H. Dach, M. Rumeau, H. Buisson, J. Schrotter, Water defluoridation processes: a review, Application: nanofiltration (NF) for future large-scale pilot plants, *Adv. Fluorine Sci.*, 2 (2006) 49–80.
- [22] S.S. Wadekar, R.D. Vidic, Influence of active layer on separation potentials of nanofiltration membranes for inorganic ions, *Environ. Sci. Technol.*, 51 (2017) 5658–5665.
- [23] J. Mui, J. Ngo, B. Kim, Aggregation and colloidal stability of commercially available Al₂O₃ nanoparticles in aqueous environments, *Nanomaterials*, 6 (2016) 90, doi: 10.3390/nano6050090.
- [24] B. Al-Rashdi, D. Johnson, N. Hilal, Removal of heavy metal ions by nanofiltration, *Desalination*, 315 (2013) 2–17.
- [25] Y. Boussouga, A. Lhassani, Study of mass transfer mechanisms for reverse osmosis and nanofiltration membranes intended for desalination, *J. Mater. Environ. Sci.*, 8 (2017) 1128–1138.
- [26] Y. Boussouga, A. Lhassani, Performances of nanofiltration and low pressure reverse osmosis membranes for desalination: characterization and modelling, *IOP Conf. Ser.: Mater. Sci. Eng.*, 186 (2017), doi: 10.1088/1757-899X/186/1/012039.
- [27] M. Breida, S.A. Younssi, M. El Rhazi, M. Bouhria, Removal of heavy metals by tight γ -Al₂O₃ ultrafiltration membrane at low pressure, *Desal. Water Treat.*, 167 (2019) 231–244.
- [28] Q. Li, X. Pan, Z. Qu, X. Zhao, Y. Jin, H. Dai, B. Yang, X. Wang, Understanding the dependence of contact angles of commercially RO membranes on external conditions and surface features, *Desalination*, 309 (2013) 38–45.
- [29] J.V. Nicolini, C.P. Borges, H.C. Ferraz, Selective rejection of ions and correlation with surface properties of nanofiltration membranes, *Sep. Purif. Technol.*, 171 (2016) 238–247.
- [30] Z. Chen, J. Luo, X. Hang, Y. Wan, Physicochemical characterization of tight nanofiltration membranes for dairy wastewater treatment, *J. Membr. Sci.*, 547 (2018) 51–63.
- [31] J.R. McCutcheon, M. Elimelech, Influence of membrane support layer hydrophobicity on water flux in osmotically driven membrane processes, *J. Membr. Sci.*, 318 (2008) 458–466.
- [32] B. Han, S. Liang, B. Wang, J. Zheng, X. Xie, K. Xiao, X. Wang, X. Huang, Simultaneous determination of surface energy and roughness of dense membranes by a modified contact angle method, *Colloids Surf., A*, 562 (2019) 370–376.
- [33] V. Gekas, K.M. Persson, M. Wahlgren, B. Sivik, Contact angles of ultrafiltration membranes and their possible correlation to membrane performance, *J. Membr. Sci.*, 72 (1992) 293–302.
- [34] T. Chau, W. Bruckard, P. Koh, A. Nguyen, A review of factors that affect contact angle and implications for flotation practice, *Adv. Colloid Interface Sci.*, 150 (2009) 106–115.
- [35] F. Wang, C.S. Wong, D. Chen, X. Lu, F. Wang, E.Y. Zeng, Interaction of toxic chemicals with microplastics: a critical review, *Water Res.*, 139 (2018) 208–219.
- [36] P. Goh, A. Ismail, A review on inorganic membranes for desalination and wastewater treatment, *Desalination*, 434 (2018) 60–80.
- [37] M. Reig, E. Licon, O. Gibert, A. Yaroshchuk, J.L. Cortina, Rejection of ammonium and nitrate from sodium chloride solutions by nanofiltration: effect of dominant-salt concentration on the trace-ion rejection, *Chem. Eng. J.*, 303 (2016) 401–408.
- [38] M.J. López-Muñoz, A. Sotto, J.M. Arsuaga, B. Van der Bruggen, Influence of membrane, solute and solution properties on the retention of phenolic compounds in aqueous solution by nanofiltration membranes, *Sep. Purif. Technol.*, 66 (2009) 194–201.
- [39] P. Monash, A. Majhi, G. Pugazhenth, Separation of bovine serum albumin (BSA) using γ -Al₂O₃-clay composite ultrafiltration membrane, *J. Chem. Technol. Biotechnol.*, 85 (2010) 545–554.
- [40] J. Luo, L. Ding, Influence of pH on treatment of dairy wastewater by nanofiltration using shear-enhanced filtration system, *Desalination*, 278 (2011) 150–156.
- [41] J. Lee, J.-H. Ha, I.-H. Song, Improving the antifouling properties of ceramic membranes via chemical grafting of organosilanes, *Sep. Sci. Technol.*, 51 (2016) 2420–2428.
- [42] A.E. Childress, M. Elimelech, Relating nanofiltration membrane performance to membrane charge (electrokinetic) characteristics, *Environ. Sci. Technol.*, 34 (2000) 3710–3716.
- [43] A. Santafé-Moros, J. Gozálviz-Zafrilla, J. Lora-García, Nitrate removal from ternary ionic solutions by a tight nanofiltration membrane, *Desalination*, 204 (2007) 63–71.
- [44] R. Benalla, M. Persin, N. Toreis, J. Sarrazin, A. Larbot, A. Bouhaouss, Rétention de sels simples par une membrane chargée d'ultrafiltration à base d'alumine gamma, *J. Chim. Phys. Phys. Chim. Biol.*, 96 (1999) 1387–1399.
- [45] R. Shang, A.R. Verliefe, J. Hu, Z. Zeng, J. Lu, A.J. Kemperman, H. Deng, K. Nijmeijer, S.G. Heijman, L.C. Rietveld, Tight ceramic UF membrane as RO pre-treatment: the role of electrostatic interactions on phosphate rejection, *Water Res.*, 48 (2014) 498–507.
- [46] H. Krieg, S. Modise, K. Keizer, H. Neomagus, Salt rejection in nanofiltration for single and binary salt mixtures in view of sulphate removal, *Desalination*, 171 (2005) 205–215.
- [47] J. Luo, Y. Wan, Effects of pH and salt on nanofiltration – a critical review, *J. Membr. Sci.*, 438 (2013) 18–28.
- [48] Z. Wang, Y.-M. Wei, Z.-L. Xu, Y. Cao, Z.-Q. Dong, X.-L. Shi, Preparation, characterization and solvent resistance of γ -Al₂O₃/ α -Al₂O₃ inorganic hollow fiber nanofiltration membrane, *J. Membr. Sci.*, 503 (2016) 69–80.
- [49] R. Bahar, M. Hawlader, L.S. Woei, Performance evaluation of a mechanical vapor compression desalination system, *Desalination*, 166 (2004) 123–127.
- [50] B. Van der Bruggen, C. Vandecasteele, Removal of pollutants from surface water and groundwater by nanofiltration: overview of possible applications in the drinking water industry, *Environ. Pollut.*, 122 (2003) 435–445.
- [51] D.L. Oatley, L. Llenas, R. Pérez, P.M. Williams, X. Martínez-Lladó, M. Rovira, Review of the dielectric properties of nanofiltration membranes and verification of the single oriented layer approximation, *Adv. Colloid Interface Sci.*, 173 (2012) 1–11.
- [52] A.B. Nasr, C. Charcosset, R.B. Amar, K. Walha, Defluoridation of water by nanofiltration, *J. Fluorine Chem.*, 150 (2013) 92–97.
- [53] L. Bruni, S. Bandini, The role of the electrolyte on the mechanism of charge formation in polyamide nanofiltration membranes, *J. Membr. Sci.*, 308 (2008) 136–151.

- [54] F. Garcia, D. Ciceron, A. Saboni, S. Alexandrova, Nitrate ions elimination from drinking water by nanofiltration: membrane choice, *Sep. Purif. Technol.*, 52 (2006) 196–200.
- [55] F. Abidar, A. Soudani, M. Morghi, M. Chiban, M. Zerbet, F. Sinan, Removal of by (cordierite/ZrO₂) membrane modified by microparticles, *Desal. Water Treat.*, 57 (2016) 17473–17482.
- [56] L. Paugam, S. Taha, G. Dorange, P. Jaouen, F. Quéméneur, Mechanism of nitrate ions transfer in nanofiltration depending on pressure, pH, concentration and medium composition, *J. Membr. Sci.*, 231 (2004) 37–46.
- [57] K.L. Tu, L.D. Nghiem, A.R. Chivas, Coupling effects of feed solution pH and ionic strength on the rejection of boron by NF/RO membranes, *Chem. Eng. J.*, 168 (2011) 700–706.
- [58] C.K. Diawara, Nanofiltration process efficiency in water desalination, *Sep. Purif. Rev.*, 37 (2008) 302–324.
- [59] M. Nilsson, G. Trägårdh, K. Östergren, The influence of pH, salt and temperature on nanofiltration performance, *J. Membr. Sci.*, 312 (2008) 97–106.
- [60] J. Luo, Y. Wan, Effect of highly concentrated salt on retention of organic solutes by nanofiltration polymeric membranes, *J. Membr. Sci.*, 372 (2011) 145–153.